

Far tails of the biased CTRW model under the short time limit

Wanli Wang, Kaixin Zhang and Yuda Cheng

School of Mathematical Sciences, Zhejiang University of Technology, Hangzhou 310023, China

(Dated: January 21, 2026)

It has been observed in numerous experiments, simulations, and various theoretical treatments that the spreading of particles can be modeled by the continuous-time random walk. We consider two well-known cases, i.e., Gaussian displacements and discrete displacements, to compute the position distribution and demonstrate the emergence of exponential decay in the far tails when a bias is introduced. We further analyze the temporal rate function and the positional rate function to examine the convergence of the theoretical predictions. For Gaussian displacements, we further discuss the relationship between the position distributions with and without bias in different asymptotic limits.

I. INTRODUCTION

Brownian motion refers to the random walk of particles suspended in a fluid or gas, arising from their collisions with the fast-moving molecules in the medium. This phenomenon was first observed in 1872 when pollen from the plant *Clarkia pulchella* was immersed in water. From early studies, we now understand Brownian motion as the continuum limit of a Pearson walk or Wiener process from a mathematical perspective. It is well-known that the position follows a Gaussian distribution, and that the mean squared displacement increases linearly with the observation time t in the long-time limit. The former is a direct consequence of the central limit theorem, which states that the properly normalized sum of a sequence of independent and identically distributed (IID) random variables converges to a normal distribution, describing the behavior of the central part of the distribution. By contrast, what happens in the short-time regime, for example, $t = 1/2$? When the observation time is very short, most particles remain effectively trapped by their initial conditions. Consequently, we are not concerned with the statistics of typical fluctuations. Instead, we focus on the decay of the far tails of the position distribution, which is closely related to large deviations theory [1–6].

To be more exactly, in Ref. [7] Chaudhuri, Berthier, and Kob study the distribution of single particle displacements in a broad class of materials close to the glass, where they found that the tails follow exponential, rather than Gaussian, decay based on continuous-time random walk (CTRW) model [8–12]. The novelty is found in many systems or experiments, including mRNA molecules in heterogeneous environments [13], nano-particles in confined diffusion [14] and in nanopost array [15], a tracer particle in crowded media [16], living cells [17], stock market [18] and diffusion of heterogeneous populations [19], the motion of Chloroplasts in plant cells [20]; see related works in Refs. [7, 14, 17, 19, 21–31]. Recently, Barkai and Burov found that exponential behavior is generally valid in a large class of problems of transport provided that the PDF of waiting time between two successive steps is analytic at small τ [32]. The anti-bunching and bunching of jump events were discussed to study large deviations of the position [33]. Pacheco-

Pozo and Sokolov investigated rate functions within the framework of large deviation theory for a broad class of waiting-time distributions, ranging from the exponential distribution to the one-sided Lévy distribution [34]. In the context of the CTRW model, super-exponential and sub-exponential displacements were investigated using the large deviations theory and the single big jump principle [35]. Besides, the exponential decay was discussed in terms of diffusing diffusivity models [30, 36].

When a bias is introduced, the system exhibits a range of intriguing behaviors. Notably, the introduction of bias leads to a nontrivial relationship between the position distributions in the biased and unbiased cases, revealing interesting statistical structures and dynamic properties [37]. This investigation led to the identification of an exponential decay in the positional distribution using the relationship between the positional distribution with and without bias, and the detailed balanced assumption. In this manuscript, we present additional investigations for this phenomenon and extend our discussions to encompass scenarios that were not previously explored in [37].

As mentioned in [38, 39], the large deviation principle is caused by many jumps moving in the same direction with its characteristic exponential decay. For a finite time t , many short waiting times between two successive jumps are responsible for the mentioned large deviations. Note that the single big jump principle discussed in [40–43] is also related to large deviations or rare fluctuations, but their observables are investigated in the long time limit.

This manuscript is organized as follows. In Sect. II we introduce the CTRW model. The far tails of the distribution and the rate functions are investigated in Sect. III using the large deviation theorem for the Gaussian displacements. In Sect. IV, we consider the binomial random walk and the far tails of the positional distribution. Finally, we conclude with a discussion.

II. MODEL

In the CTRW model, the position of the random walker, $x(t) = \sum_{i=1}^N x_i$, is determined by the distribution of waiting times and displacements, respectively. Here, N

is a t -dependent random integer representing the number of jumps occurring from time 0 to time t . The particle is on the origin at time $t = 0$ and waits at its initial position for a random time τ_1 drawn from a PDF $\phi(\tau)$. After that, the particle immediately makes a jump of x_1 with PDF $f(x)$. At time $t = \tau_1$, we generate a new waiting time τ_2 and a displacement x_2 according to the corresponding PDFs $\phi(\tau)$ and $f(x)$, respectively. Then, the process is renewed. Here, the waiting time τ_i and the displacement x_i are mutually IID random variables. All along the manuscript, x_0 denotes the particle's initial position; in our setting, $x_0 = 0$.

Let $f(x|N)$ [44, 45] be the probability that N steps are made in the time interval $(0, t)$. Let $P(x, t)$ be the PDF of finding the particle at x at time t . The density of the spreading particles is

$$\begin{aligned} P(x, t) &= \sum_{N=0}^{\infty} Q_t(N) f(x|N) \\ &\rightarrow \int_0^{\infty} Q_t(N) f(x|N) dN, \end{aligned} \quad (1)$$

where N is treated as a continuous variable. Assuming the displacements of the particle are IID random variables, so $\tilde{f}(k|N) = \hat{f}^N(k)$ with $\hat{f}(k) = \int_{-\infty}^{\infty} \exp(ikx) f(x) dx$ being the Fourier transform of $f(x)$. In Laplace space, the probability distribution of the number of events between 0 and t reads [44]

$$\hat{Q}_s(N) = \frac{1 - \hat{\phi}(s)}{s} \hat{\phi}^N(s), \quad (2)$$

where $\hat{\phi}(s) = \int_0^{\infty} \phi(\tau) \exp(-s\tau) d\tau$ denotes the Laplace transform of $\phi(t)$, from the real space t to the Laplace space s . In the particular case of $N = 0$, $Q_0(t) = \int_t^{\infty} \phi(\tau) d\tau$ is the survival probability.

As given in [32], the nearly exponential decay of the number of renewals is universal, holding in general and under mild conditions. Mathematically, $\phi(\tau)$ should be analytic at the critical point $\tau = 0$. In other words, in the short time limit ($\tau \rightarrow 0$), Taylor's expansion of $\phi(\tau)$ can be shown as [32]

$$\phi(\tau) \sim \sum_{j=0}^{\infty} C_{A+j} \tau^{A+j}, \quad \tau \rightarrow 0, \quad (3)$$

where $A \geq 0$ is a positive integer. Note that the parameter A can be extended to the case when $A > -1$. For further details, see Ref. [46]. In our simulations, we use a well-known waiting time PDF called the exponential distribution

$$\phi(\tau) = \exp(-\tau), \quad (4)$$

where waiting times τ have a finite mean and variance. According to Eq. (3), we have $A = 0$, $C_0 = 1$, and $C_1 =$

-1 . A broad distribution will be discussed here, namely, the Dagum distribution

$$\phi(\tau) = \frac{1}{(1 + \tau)^2}. \quad (5)$$

It implies that both the mean and the variance of τ are infinite. When $\tau \rightarrow 0$, the Taylor expansion of the Dagum distribution yields $\phi(\tau) \sim 1 - 2\tau$. Therefore, from Eq. (3), it follows that $A = 0$, $C_A = 1$, and $C_{A+1} = -2$.

For large N , using Eqs. (2) and (3), the far tail of renewals behaves as [32]

$$Q_t(N) \sim \frac{\exp\left(\frac{C_{A+1}}{C_A} t + N(A+1) \ln\left(\frac{tze}{N}\right)\right)}{\sqrt{2\pi N(A+1)}} \quad (6)$$

with

$$z = \frac{[C_A \Gamma(A+1)]^{\frac{1}{1+A}}}{(A+1)}. \quad (7)$$

Note that the leading term, corresponding to the bracketed expression in Eq. (6), is $N(A+1) \ln(tze/N)$, indicating that the far tail of the distribution of N exhibits a nearly exponential decay. In what follows, Eq. (6) will serve as an important tool for analyzing the far-tail behavior of the position distribution discussed in the manuscript.

III. EXPONENTIAL TAILS OF THE DISTRIBUTION OF THE POSITION WITH GAUSSIAN DISPLACEMENTS

We begin with a scenario where the PDF of the waiting time exhibits analytic behavior as τ approaches zero and the step length follows a Gaussian distribution. Subsequently, we analyze the far tails of the positional distribution, explore the Einstein-like relation, and examine the rate function.

A. Far tails of the positional distribution

For the displacement, we focus on a Gaussian distribution with the mean $a > 0$ and the variance σ^2

$$f(x) = \frac{1}{\sqrt{2\pi\sigma^2}} \exp\left[-\frac{(x-a)^2}{2\sigma^2}\right]. \quad (8)$$

As noted earlier, we assume displacements x are IID random variables. For a given N , the probability density $f(x|N)$ follows

$$f(x|N) = \frac{1}{\sqrt{2\pi\sigma^2 N}} \exp\left(-\frac{(x-aN)^2}{2\sigma^2 N}\right). \quad (9)$$

According to Eq. (1), we have

$$P(x, t) \sim \int_0^\infty \exp \left(-N \underbrace{\left[\left(\frac{x/N - a}{\sqrt{2\sigma^2}} \right)^2 - (A+1) \ln \left(\frac{zte}{N} \right) - \frac{C_{A+1}}{C_A} \frac{t}{N} + \frac{\ln(2\pi\sigma^2 N \sqrt{A+1})}{N} \right]}_{\chi(N)} \right) dN. \quad (10)$$

For Eq. (10), we used the large deviation result for the number of renewals [32], namely Eq. (6). In turn, this means that Eq. (10) is valid for large x since the mean and variance of displacements are finite. Generally, it is not easy to perform the integral to get an analytic solution. Here we turn to the Cramér-Daniels approach [47] (sometimes called the saddle point approximation), and apply it to our problem. For a large $|x|$, from the saddle point method and Eq. (10), the far tails of the positional distribution are

$$P(x, t) \sim \frac{\sqrt{2\pi}}{\sqrt{|\chi''(N^*)|}} \exp(-\chi(N^*)), \quad (11)$$

where the saddle point N^* satisfies $\chi'(N^*) = 0$, namely

$$\frac{a^2}{\sigma^2} - 2(A+1) \ln \left(\frac{tz}{N^*} \right) - \frac{x^2}{(N^*)^2 \sigma^2} + \frac{1}{N^*} = 0. \quad (12)$$

In the large N^* limit, the asymptotic solution of Eq. (12) reads

$$N^* \sim \frac{|x|}{\sigma \sqrt{(A+1) W_0 \left[\frac{(A+1) \exp \left(\frac{a^2}{(A+1)\sigma^2} \right) x^2}{(C_A \Gamma(A+1))^{\frac{2}{A+1}} \sigma^2} \frac{t^2}{t^2} \right]}}, \quad (13)$$

where $W_0(y)$ is the principal branch of a Lambert W function [48–50], also called the product logarithm function. When $|x| \rightarrow \infty$, Eq. (13) reduces to

$$N^* \propto \frac{|x|}{\sigma \sqrt{(A+1) \ln(\exp(\frac{a^2}{(A+1)\sigma^2}) \frac{x^2}{t^2})}}. \quad (14)$$

An interesting feature of N^* is exclusively exhibited by the large deviation analysis, i.e., when the force increases, N decreases. This phenomenon can be explained as follows: When the bias is strong, the particle requires fewer steps to reach a fixed position than when the bias is weak. Let N^- and N^+ be the number of steps of the particle reaching the site $-|x|$ and $|x|$, respectively. Clearly, N^+ and N^- are dependent on a and σ . While $|x| \gg \langle x(t) \rangle$, position-dependent N^+ and N^- is the same based on Eq. (14); see Fig. 1. For a fixed a and $x \rightarrow \infty$, Eq. (14) yields

$$\frac{N^*}{|x|} \sqrt{\ln \left(\frac{|x|}{t} \right)} \propto \frac{1}{\delta \sqrt{2(A+1)}}, \quad (15)$$

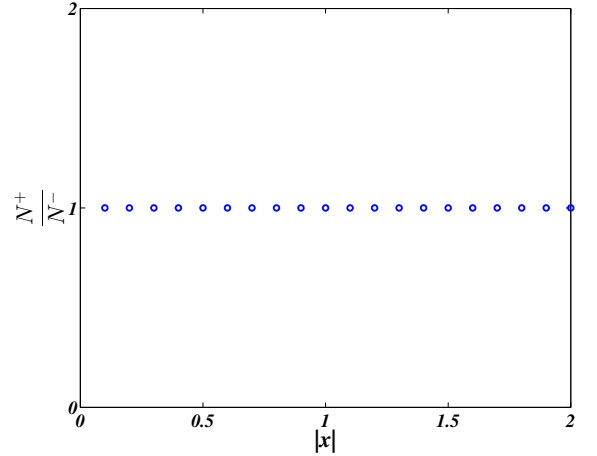


FIG. 1: Plot of the ratio of N^+ and N^- versus x with the waiting time following exponential distribution $\phi(\tau) = \exp(-\tau)$. The symbols illustrate the exact result from Eq. (1). We find $P_N(x, t) = Q_t(N) f(x|N)$ then choose the maximum of $P_N(x, t)$ for a given x , finally, we record the corresponding N^+ or N^- for positive or negative x , respectively. Here we choose $\sigma = 0.1$, $a = 0.01$, and $t = 2$.

tending to a constant.

According to Eq. (11), we find the main result of this section

$$P(x, t) \sim \frac{1}{\sqrt{2\pi\sigma(A+1)^{3/2}}} \times \frac{\exp \left(\frac{a}{\sigma^2} x + \frac{C_{A+1}}{C_A} t - |x| G \left(\frac{x}{t} \right) \right)}{\sqrt{\left| |x| \left(\sqrt{W_0 \left(\frac{gx^2}{t^2} \right)} + \frac{1}{\sqrt{W_0 \left(\frac{gx^2}{t^2} \right)}} \right) - \sigma \right|}} \quad (16)$$

with

$$G(l) = \frac{\sqrt{A+1}}{\sigma} \left(\sqrt{W_0(gl^2)} - \frac{1}{\sqrt{W_0(gl^2)}} \right)$$

and

$$g = \frac{\exp(\frac{a^2}{(1+A)\sigma^2})}{(1+A)\sigma^2 z^2}. \quad (17)$$

When a bias is added, the two exponential tails become asymmetric. Specifically, the right tail is $\exp(-ax/\sigma^2)$

times larger than the left if $a > 0$. Note that there is a term $a/\sigma^2 x$ on the numerator of Eq. (16), which indicates that one of the tails decays rapidly if the bias is strong.

Based on Eq. (16), the asymptotic behavior of the position is

$$P(x, t) \propto \exp \left(-x \text{sign}(x) G(l) + \frac{a}{\sigma^2} x + \frac{C_{A+1}}{C_A} \right). \quad (18)$$

It demonstrates that the far tails of the distribution of the position decay like an exponential function instead of a Gaussian distribution since $W_0(|y|)$ increases as $\ln(|y|)$ for large $|y|$. What we would like to mention is that the statistics of the tails of waiting time PDFs are not important at all and the tails of the positional distribution are simply determined by the Taylor expansion at small τ .

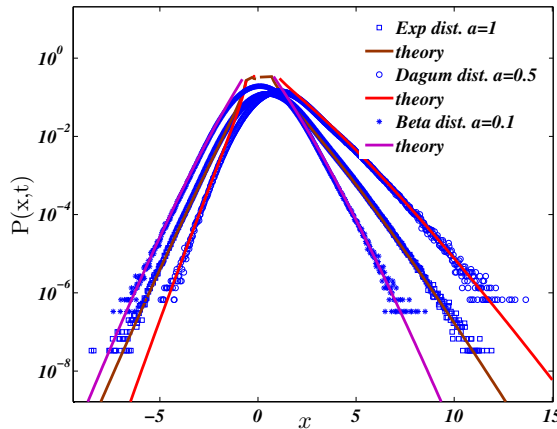


FIG. 2: The positional distribution exhibits asymmetric exponential tails for different biases, considering various waiting time PDFs, such as exponential distribution $\phi(\tau) = \exp(-\tau)$ (' \square '), Dagum distribution $\phi(\tau) = 1/(1+\tau)^2$ (' \circ ') and a special form of Beta distribution $\phi(\tau) = 6\tau(1-\tau)$ (' $*$ '). The symbols represent simulations generated from 10^9 trajectories and the solid lines depict theoretical predictions based on Eq. (16). Note that Throughout we did not discuss the non-moving particles. In our setting, we choose $\sigma = 1$ and $t = 0.5$ for different a .

B. Einstein-like relation

We delve deeper into the far tails of the positional distribution and explore the impact of the bias. Inspired

by the Einstein relation [51–54] describing the relation between the mean of the position with the bias and the variance of the position without bias, we aim to investigate the ratio of the positional PDF with and without bias. Based on Eq. (16), we have

$$\frac{P(x, t)_{a \neq 0}}{P(x, t)_{a=0}} \sim \exp \left(\frac{a}{\sigma^2} x - x \text{sign}(x) \right. \\ \left. \times \left[G \left(\frac{x}{t} \right)_{a \neq 0} - G \left(\frac{x}{t} \right)_{a=0} \right] \right). \quad (19)$$

Note that Eq. (19) is valid for large $|x|$ under study. Rewriting the above equation, we find

$$\ln \left(\frac{P(x, t)_{a \neq 0}}{P(x, t)_{a=0}} \right) \sim \frac{a}{\sigma^2} x - x \text{sign}(x) \\ \times \left[G \left(\frac{x}{t} \right)_{a \neq 0} - G \left(\frac{x}{t} \right)_{a=0} \right], \quad (20)$$

which is plotted by the red solid lines in Fig. 3. An interesting limit involving a could have significant practical applications. Recall that $G(x/t)$ is an even function concerning bias a . Therefore, Taylor's series of $G(x/t)$ with respect to small a can be expressed as follows

$$G \left(\frac{x}{t} \right) = G \left(\frac{x}{t} \right)_{a=0} + \frac{1}{2!} \frac{d^2 G \left(\frac{x}{t} \right)}{da^2} a^2 + \dots \quad (21)$$

From Eq. (21), we can see that for a small bias, the right side of Eq. (20) increases roughly in proportion to x . It indicates that the leading term of the right-hand side of Eq. (19) for small a is

$$\frac{P(x, t)_{a \neq 0}}{P(x, t)_{a=0}} \sim \exp \left(\frac{a}{\sigma^2} x \right) \quad (22)$$

or

$$\ln \left(\frac{P(x, t)_{a \neq 0}}{P(x, t)_{a=0}} \right) \sim \frac{a}{\sigma^2} x; \quad (23)$$

see the dashed line in Fig. 3. When the parameter a increases, correction terms in Eq. (21), such as a^2 and a^4 , come into play. It indicates that Eqs. (22) and (23) become ineffective. For that, we still assume that the bias is weak, but the correction term is added relative to Eq. (22). From Eq. (19), we get a useful expression

$$\frac{P(x, t)_{a \neq 0}}{P(x, t)_{a=0}} \sim \exp \left[\frac{ax}{\sigma^2} - \frac{\sqrt{A+1}|x|}{\sigma} \sqrt{W_0 \left(\frac{(\frac{x}{t})^2}{(A+1)\sigma^2 z^2} \right)} \left(\sqrt{\frac{a^2}{((A+1)\sigma^2) W_0 \left(\frac{(\frac{x}{t})^2}{(A+1)\sigma^2 z^2} \right)}} + 1 - 1 \right) \right]. \quad (24)$$

If we replace the terms in the last parentheses by their equivalent values, then in the limit of large $|x|$, Eq. (24) reduces to:

$$\ln \left(\frac{P(x, t)_{a \neq 0}}{P(x, t)_{a=0}} \right) \sim \frac{ax}{\sigma^2} - \frac{a^2 |x|}{2\sigma^3 \sqrt{A+1}} \frac{1}{\sqrt{W_0 \left(\frac{x^2}{(A+1)\sigma^2 z^2 t^2} \right)}}. \quad (25)$$

The last term on the right-hand side of Eq. (25) approaches a constant as $|x|$ becomes small. For small x , the function $W_0(|x|)$ can be approximated as $|x|$. If $|x| \rightarrow \infty$, the second term grows as $|x|/\ln(|x|)$, becoming significant for large $|x|$. This explains why the dominant term is effective for weak bias. See the dotted line in Fig. 3.

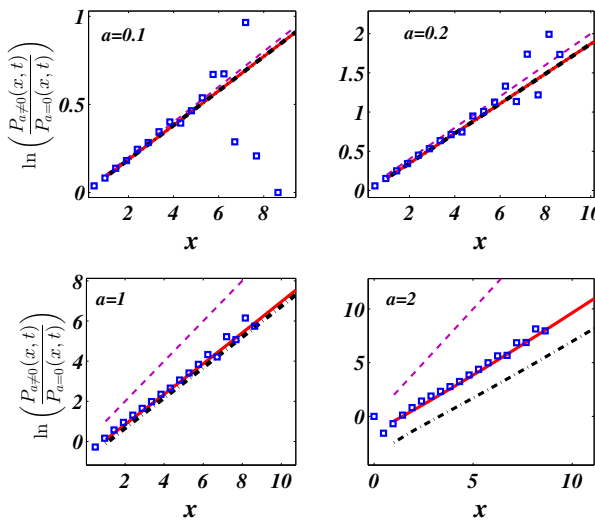


FIG. 3: Plot of $\ln \left(\frac{P(x, t)_{a \neq 0}}{P(x, t)_{a=0}} \right)$ versus the position x for different variables a where waiting times are drawn from Dagum distribution $\phi(\tau) = 1/(1+\tau)^2$. The red solid lines correspond to the theoretical result given by Eq. (19), which is valid for all types of biases. The corresponding asymptotic behavior, as described by Eq. (25), is shown by the dash-dotted lines for a weak bias. The linear relation, given by Eq. (23), is represented by the dashed lines. The symbols are simulations generated from 10^8 realizations with $\sigma = 1$. The figure shows that as we decrease a , the linear relationship Eq. (23) becomes readily detected.

C. Rate function

The central limit theorem states that when independent random variables are added, their properly normalized sum approaches a normal distribution as the sample size increases. Instead of focusing on the central part of the distribution described by the central limit theorem, our interests lie in the statistical behavior of the far tails using large deviation theories. The rate function [3, 38, 55] is called the Cramér function or sometimes the “entropy function”, which is widely used to quantify the probabilities of rare events. In this context, we consider two types of rate functions, one associated with the position and the other with the time. While the main idea remains the same for both approaches, the only distinction lies in the limit being considered, namely $x \rightarrow \infty$ or $t \rightarrow \infty$.

Utilizing Eq. (16), we have

$$P(x, t) \sim \exp \left(-|x|G \left(\frac{x}{t} \right) + \frac{a}{\sigma^2}x + \frac{C_{A+1}}{C_A}t \right). \quad (26)$$

Rewriting Eq. (26), the rate function with respect to x follows

$$\lim_{t \rightarrow \infty} \frac{\ln(P(x, t))}{-|x|} = \mathcal{I}_x \left(l = \frac{x}{t} \right) \quad (27)$$

with

$$\mathcal{I}_x(l) = G(l) - \frac{a}{\sigma^2} \text{sign}(l) - \frac{C_{A+1}}{C_A} \frac{1}{|l|}. \quad (28)$$

Note that for large l the asymptotic behavior of Eq. (28) is

$$\mathcal{I}_x(l) \sim \frac{\sqrt{A+1}}{\sigma} \sqrt{\ln(gl^2)}, \quad (29)$$

which is responsible for the nearly exponential decay of the positional distribution. As shown in Fig. 4, the rate function $\mathcal{I}_x(l)$ goes to infinity when $l \rightarrow 0$. On the other hand, when $l \rightarrow \infty$, Eq. (29) also approaches infinity, but at an extremely slow rate.

Similarly, the (time) rate function follows

$$\lim_{t \rightarrow \infty} \frac{\ln(P(x, t))}{-t} = \mathcal{I}_t \left(l = \frac{x}{t} \right) \quad (30)$$

with $\mathcal{I}_t(l) = \text{sign}(l)l\mathcal{I}_x(l)$, where we got the time rate function using the positional rate function Eq. (27) without losing the other information.

Next, we discuss the case of small $|l|$. For $|l| \rightarrow 0$, Eq. (28) simplifies to

$$\begin{aligned} \mathcal{I}_x(l) &= -\frac{\sqrt{A+1}}{\sigma} \frac{1}{\sqrt{gl^2}} + \frac{\sqrt{A+1}\sqrt{gl^2}}{\sigma} \\ &\quad - \frac{a}{\sigma^2} \text{sign}(l) - \frac{C_{A+1}}{C_A} \frac{1}{|l|}. \end{aligned} \quad (31)$$

Combining Eqs. (16) and (31), we have

$$\begin{aligned} P(x, t) &\simeq \exp \left(\frac{a}{\sigma^2} x + \frac{\sqrt{A+1}}{\sqrt{g}\sigma} t - \frac{\sqrt{A+1}\sqrt{g}}{(2\sigma)} \frac{x^2}{t} \right. \\ &\quad \left. + \frac{C_{A+1}}{C_A} t \right). \end{aligned} \quad (32)$$

The above form corresponds to the Gaussian law, consistent with the central limit theorem.

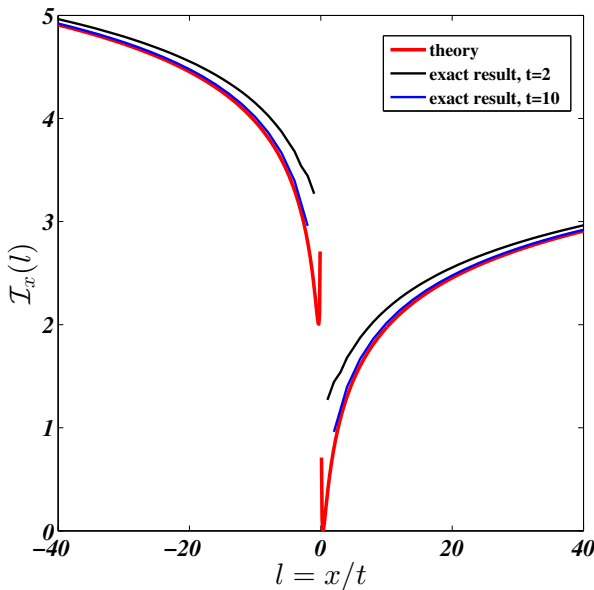


FIG. 4: Rate function $\mathcal{I}_x(l)$ plotted for different times t . Here, the waiting time follows the Erlang distribution $\phi(\tau) = \tau^2 \exp(-\tau)/2$ with the mean 3. In that sense $A = 2$, $C_2 = 1/2$ and $C_3 = -C_2$. The red solid line is the theoretical prediction (27) without fitting. The exact results plot $\ln(P(x, t)/(-|x|))$, where $P(x, t)$ is estimated from Eq. (1) using the infinite terms [33]. In our setting $a = 1$ and $\sigma = 1$. Though the observation time t is not very long, the convergence to the exact result is fast.

IV. BINOMIAL RANDOM WALK

In the previous section, we considered the case of continuous displacements; now we turn to the discrete case. Let's examine a scenario of a random walk on a one-dimensional lattice, commencing from position zero. Suppose a step to the right occurs with probability p ,

while a leftward step has the probability $q = 1 - p > 0$. The particle is only allowed to walk on the sites $j = \dots, -3, -2, -1, 0, 1, 2, 3, \dots$. Let the step length be one. This concept was introduced into science by Karl Pearson in a letter to Nature [56]. Mathematically, the displacement follows

$$f(x) = \begin{cases} 1, & \text{probability } p \text{ to the right;} \\ -1, & \text{probability } q = 1 - p \text{ to the left} \end{cases} \quad (33)$$

with $0 < p < 1$. In particular, if $p = 1/2$, it means that the particles have an equal probability of jumping left and right, i.e., a symmetric case. Note that p and q are independent of the site $j = \dots, -2, -1, 0, 1, \dots$. The probability of arriving at site j after N steps, denoted as $f(x|N)$, follows

$$f(x|N) = \frac{N!}{(\frac{N+x}{2})!(\frac{N-x}{2})!} p^{\frac{N+x}{2}} q^{\frac{N-x}{2}}, \quad |x| \leq N. \quad (34)$$

It indicates that the particles can not reach sites larger than N as the length of the displacement is one and the number of steps is N . It is important to note that for an even value of N , the probability of reaching an odd-numbered site x is zero, and the same applies to odd values of N . Using Stirling's approximation $n! \sim \sqrt{2\pi n}(n/e)^n$, Eq. (34) reduces to

$$f(x|N) \sim \frac{(2N)^{N+\frac{1}{2}}}{\sqrt{\pi}} \frac{p^{\frac{N+x}{2}} q^{\frac{N-x}{2}}}{(N+x)^{\frac{N+x+1}{2}} (N-x)^{\frac{N-x+1}{2}}}. \quad (35)$$

Rewriting Eq. (34), we have

$$\begin{aligned} f(x|N) &\sim \frac{1}{\sqrt{\pi}} 2^{N+\frac{1}{2}} N^{N+\frac{1}{2}} (N-x)^{\frac{1}{2}(-N+x-1)} \\ &\quad \times (N+x)^{\frac{1}{2}(-N-x-1)} p^{\frac{N+x}{2}} q^{\frac{N-x}{2}}, \end{aligned} \quad (36)$$

which will be used to investigate the tails of the distribution of positions. Based on Eq. (36), the following two limiting laws are easy to get:

$$f(x|N) \sim \frac{2^{N+\frac{1}{2}} (pq)^{\frac{N}{2}}}{\sqrt{\pi}} \frac{1}{\sqrt{N}} \quad (37)$$

for $x \rightarrow 0$, and

$$f(x|N) \sim \frac{p^{\frac{N+x}{2}}}{\sqrt{\pi}} \quad (38)$$

when $x \rightarrow N$. For example, if $x = N$, we have $f(x|N) = p^N$, whose order is consistent with Eq. (38). Note that the deviations, i.e., the prefactor $1/\sqrt{\pi}$, stems from the term $((N-x)/2)!$ given in Eq. (37) when using Stirling's approximation. In the log-linear scale, the prefactor $1/\sqrt{\pi}$ of Eq. (38) can be ignored. Below, we start from the exponential waiting time PDF and then consider a more general one given by Eq. (3).

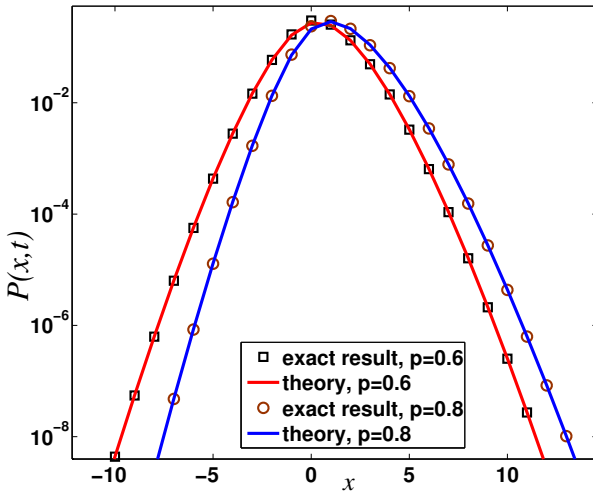


FIG. 5: Decay of the positional distribution, where waiting times are drawn from the exponential distribution $\phi(\tau) = \exp(-\tau)$ and the displacements are generated from Eq. (33). The symbols describe the exact result for various p , obtained from Eq. (1), and the solid lines are the corresponding theoretical prediction Eq. (46). The observation time is $t = 2$.

A. Exponential waiting time PDF

Let us start from the exponential distribution Eq. (4) with mean 1. From Eq. (1), for IID displacements, we have

$$\tilde{P}(k, t) = \sum_{N=0}^{\infty} Q_t(N) \tilde{f}(k)^N. \quad (39)$$

Recall that the PDF of the number of renewals follows a Poisson distribution, i.e., $Q_t(N) = \exp(-t)t^N/N!$. Summing the infinite terms, Eq. (39) yields

$$\begin{aligned} \tilde{P}(k, t) &= \exp(t(\tilde{f}(k) - 1)) \\ &= \exp(tp \exp(ik) + tq \exp(-ik) - t). \end{aligned} \quad (40)$$

We further introduce the moment-generating function, which is the expectation of a function of the random variable. Mathematically, it can be written as $K(u) = \langle \exp(ux) \rangle = \int_{-\infty}^{\infty} P(x, t) \exp(ux) dx$. Replacing $k = -iu$, from Eq. (40) the moment generating function reads

$$K(u) = tp \exp(u) + tq \exp(-u) - t. \quad (41)$$

For a more detailed explanation of the moment-generating function $K(u)$ used in the theory of large deviations, refer to Ref. [33]. Instead of performing inverse Fourier transform on Eq. (40), the saddle point approximation yields the large deviation expression [47]

$$P(x, t) \sim \frac{1}{\sqrt{2\pi K''(u^*)}} \exp(K(u^*) - u^*x), \quad (42)$$

where u^* is the solution of $K'(u^*) = x$. Based on Eq. (41), the solution of $K'(u^*) = x$ reads

$$u^* = \ln \left(\frac{x + \sqrt{4pqt^2 + x^2}}{2pt} \right). \quad (43)$$

The other solution u^* ,

$$u^* = \ln \left(\frac{x - \sqrt{4pqt^2 + x^2}}{2pt} \right), \quad (44)$$

does not satisfy the original equation. In addition, from Eqs. (41) and (43), we get

$$K''(u^*) = \sqrt{4pqt^2 + x^2} \propto |x|. \quad (45)$$

Utilizing Eqs. (42), (43), and (45), we find the far tails of the distribution of the position

$$P(x, t) \sim \frac{\exp \left(\frac{4pqt^2}{\sqrt{4pqt^2 + x^2}} - x \ln \left(\frac{\sqrt{4pqt^2 + x^2} + x}{2pt} \right) + x - t \right)}{\sqrt{2\pi|x|}}, \quad (46)$$

showing exponential decay. As plotted in Fig. 5, Eq. (46) gives an effective prediction. When $p = q = 1/2$, Eq. (46) reduces to the symmetric case discussed in [33].

Below, we consider two interesting limiting laws describing far tails. From Eq. (46), for a large and positive x , the right tail behaves as

$$P(x, t) \sim \frac{\exp \left(-x \left(\ln \left(\frac{2x}{2pt} \right) - 1 - t \right) \right)}{\sqrt{2\pi x}}, \quad (47)$$

which indicates that

$$-\frac{\ln(P(x, t))}{x} \sim \ln \left(\frac{x}{pt} \right) - 1 + \frac{t}{x} + \frac{\ln(\sqrt{2\pi x})}{x}. \quad (48)$$

It can be seen that the leading term of Eq. (48) is $\ln(x/(pt))$, which is responsible for the exponential decay of the far-right tail. Performing exp-function on both sides of Eq. (48), we get a simple expression

$$\exp \left(-\frac{\ln(P(x, t))}{x} \right) \sim \frac{x}{pt} \exp \left(\frac{\ln(\sqrt{2\pi x})}{x} - 1 + \frac{t}{x} \right). \quad (49)$$

Thus, we can see that $\exp(-\ln(P(x, t))/x)$ grows linearly with x . Namely, when x approaches infinity, the right-hand side of Eq. (49) behaves asymptotically as $x/(pt)$ for a finite duration t .

On the other hand, when $x \rightarrow -\infty$, the left tail of the distribution reads

$$P(x, t) \sim \exp(|x| + |x| \ln(qt) - |x| \ln(|x|) - t), \quad (50)$$

where we used the relations

$$\frac{x + \sqrt{x^2 + 4pqt^2}}{2pt} \sim \frac{qt}{|x|} \quad (51)$$

and

$$\frac{4pqt^2}{x + \sqrt{4pqt^2 + x^2}} \sim 2|x| \quad (52)$$

for $x \rightarrow -\infty$. To clarify, Eq. (50) demonstrates that while the left tail decays exponentially, it remains smaller than the right tail if $p > 1/2$.

B. General waiting time PDFs

In this subsection, we investigate the far tails of the positional distribution, rate functions within the context

of a general waiting time PDF.

1. Far tails of the distribution

From Eq. (1), the far tails of the position follow

$$P(x, t) \sim \sum_{N=|x|}^{\infty} \exp \left(- \underbrace{\left(\ln \left(\frac{\sqrt{\pi}(N+x)^{\frac{N+x+1}{2}}(N-x)^{\frac{N-x+1}{2}}}{(2N)^{1/2+N} p^{\frac{N+x}{2}} q^{\frac{N-x}{2}}} \right) - \frac{C_{A+1}}{C_A} t - N(A+1) \ln \left(\frac{zt}{N} \right) \right)}_{\chi(N)} \right). \quad (53)$$

Our focus is on the statistics for large x . Thus, for $Q_t(N)$, we apply Eq. (6), while for $f(x|N)$, we use Eq. (37). It is important to note that the parameter N ranges from $|x|$ to infinity for a given value of x , as each step has a length of one. Next, we apply the saddle-point approximation to estimate the infinite sum in Eq. (53). The first step is to solve for N^* , which satisfies the condition $\chi(N^*)' = 0$, i.e.,

$$\frac{(4(N^*)^2 pq) \left(\frac{tz}{N^*} \right)^{2(A+1)}}{(N^*)^2 - x^2} \sim 1. \quad (54)$$

Note that Eq. (54) is solvable for specific exceptional values of A , such as $A = 1, 2, \dots$, which correspond to cases

where the waiting time is analytic at zero. Below, we focus on the case when $A = 0$. From Eq. (54), the solution is

$$N^* \sim \sqrt{4pqt^2 z^2 + x^2}. \quad (55)$$

Increasing x increases of N^* as expected. As x becomes sufficiently large, the significance of p diminishes, and we observe that N^* is approximately equal to the absolute value of x . This linear relationship is illustrated in Fig. 6. Using the saddle point approximation, according to Eqs. (53) and (55) we find the main result of this section

$$P(x, t) \sim \frac{\sqrt{2\pi}}{\sqrt{|\chi''(N^*)|}} \exp \left(\frac{1}{4} \left(|x| \text{MM}(x, t) + \frac{4C_{A+1}}{C_A} t - 2 \ln (2\pi pqt^2 z^2) + 2x \ln(p) - 2x \ln(q) \right) \right) \quad (56)$$

with

$$\begin{aligned} \text{MM}(x, t) = & \frac{\ln (4pqt^2 z^2 + x^2)}{|x|} - 2 \left(\sqrt{\frac{4pqt^2 z^2}{x^2} + 1} + \text{sign}(x) \right) \ln \left(\sqrt{4pqt^2 z^2 + x^2} + x \right) + 4 \sqrt{\frac{4pqz^2}{x^2/t^2} + 1} \\ & + 2 \left(\text{sign}(x) - \sqrt{\frac{4pqt^2 z^2}{x^2} + 1} \right) \ln \left(\sqrt{4pqt^2 z^2 + x^2} - x \right) + 2 \sqrt{\frac{4pqt^2 z^2}{x^2} + 1} \ln (4pq(tz)^2) \\ & - \ln \left(\sqrt{2\pi} \sqrt{(A+1) \sqrt{4pqt^2 z^2 + x^2}} \right) \end{aligned} \quad (57)$$

and

$$\chi''(N^*) \sim - \frac{x^2 - 2pqt^2 z^2 \left(\sqrt{4pqt^2 z^2 + x^2} - 1 \right)}{8p^2 q^2 t^4 z^4}. \quad (58)$$

Note that $\text{MM}(x, t)$, as given in Eq. (57), is an even function with respect to x . Furthermore, the leading term of

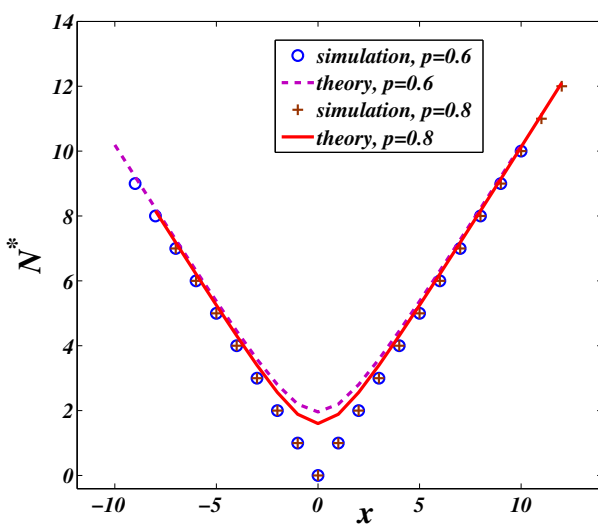


FIG. 6: Plot of N^* versus x for various p using Dagum distribution. The lines represent theoretical predictions, as expressed in Eq. (55), demonstrating a nearly linear increase concerning x . Increasing $|x|$ leads to a better convergence.

$\text{MM}(x, t)$ follows

$$\text{MM}(x, t) \sim -4 \ln(\sqrt{4pqt^2z^2 + x^2} + |x|). \quad (59)$$

Given Eqs. (56) and (59), the asymptotic behavior of the far tails of the distribution of the position is

$$P(x, t) \sim \frac{\sqrt{2\pi}}{\sqrt{|\chi''(N^*)|}} \exp\left(\frac{1}{4} \left(-4|x| \ln(\sqrt{4pqt^2z^2 + x^2} + |x|) + \frac{4C_{A+1}}{C_A} t + 2x \ln\left(\frac{p}{q}\right) \right)\right), \quad (60)$$

showing the nearly exponential decay. In addition, when $p = q = 1/2$, the distribution of the position exhibits the anticipated symmetric far tails. As illustrated in Fig. 7, the far tails are sensitive to the bias index p or q .

2. Rate functions

Now, we consider the corresponding rate functions, namely the position and the time rate functions, which

describe the limiting law for large x and large t , respectively. Rewriting Eq. (56), we have

$$P(x, t) \sim \exp\left(\frac{1}{4} \left(|x| \text{MM}(x, t) + \frac{4C_{A+1}}{C_A} t - 2 \ln(2\pi pqt^2z^2) + 2x \ln(p) - 2x \ln(q) \right) - \ln\left(\frac{\sqrt{2\pi}}{\sqrt{|\chi''(N^*)|}}\right)\right), \quad (61)$$

where $\chi''(N^*)$ is given in Eq. (58). Thus, the position rate function follows

$$\lim_{x \rightarrow \infty} \frac{P(x, t)}{-|x|} = \mathcal{I}_x \left(l = \frac{x}{t} \right) \quad (62)$$

with

$$\begin{aligned} \mathcal{I}_x \left(l = \frac{x}{t} \right) &= -\frac{1}{4} \text{MM}(lt, t) + \frac{C_{A+1}}{C_A |l|} \\ &- \frac{1}{2|l|t} + \frac{1}{2} \text{sign}(l) \ln\left(\frac{q}{p}\right) + \text{MP}(l, t) \end{aligned} \quad (63)$$

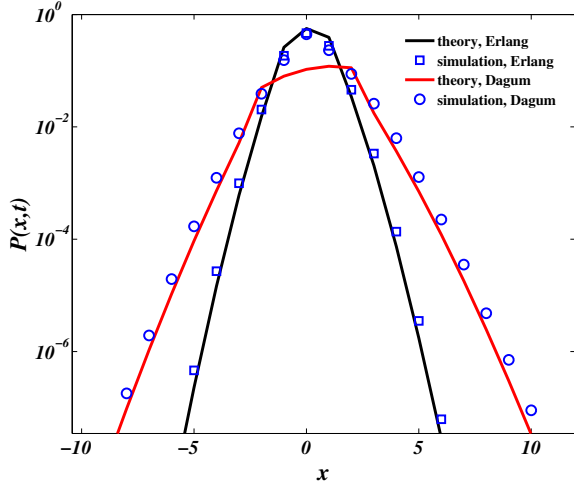


FIG. 7: The function $P(x,t)$ for cases where the jump lengths follow a discrete PDF described by Eq. (33) with different waiting times PDFs with $p = 0.6$, is shown. The theoretical approximation, i.e., Eq. (56), is described by the solid lines. The related simulations are plotted by the symbols, i.e., ‘ \square ’ for Eq. (5) and ‘ \circ ’ for $\phi(\tau) = \tau^{m-1} \exp(-\tau)/(m-1)!$ with $m = 2$.

and

$$\text{MP}(l,t) = \frac{\ln \left(\sqrt{\frac{16\pi p^2 q^2 t^4 z^4}{|x^2 - 2pqt^2 z^2 (\sqrt{4pqt^2 z^2 + x^2} - 1)|}} \right)}{|l|t}. \quad (64)$$

See the plot of Eq. (62) presented in Fig. 8. Note that the term $\ln(\sqrt{2\pi}/\sqrt{|\chi''(N^*)|})$ in Eq. (61) can be ignored when discussing rate functions, as it is not the leading term. While, in the limit of $t \rightarrow \infty$, we find the time rate function

$$\lim_{t \rightarrow \infty} \frac{P(x,t)}{-t} = \mathcal{I}_t \left(l = \frac{x}{t} \right) \quad (65)$$

with $\mathcal{I}_t(l) = l\mathcal{I}_x(l)$. See Fig. 9.

V. CONCLUSION AND DISCUSSIONS

It is well-known that when waiting times follow an exponential distribution and the displacements are drawn from a Gaussian distribution, the spreading of particles converges to a Gaussian distribution in the long-time limit. By contrast, when the observation time t is short, the positional statistics exhibit asymmetric exponential tails. In addition, we investigate the case of discrete displacements, for which the position distribution also displays an approximately exponential decay. However, the position is locked to the integers as the step length is unity. Similar to the bias-free case [32, 33], the position distribution is predominantly determined by the

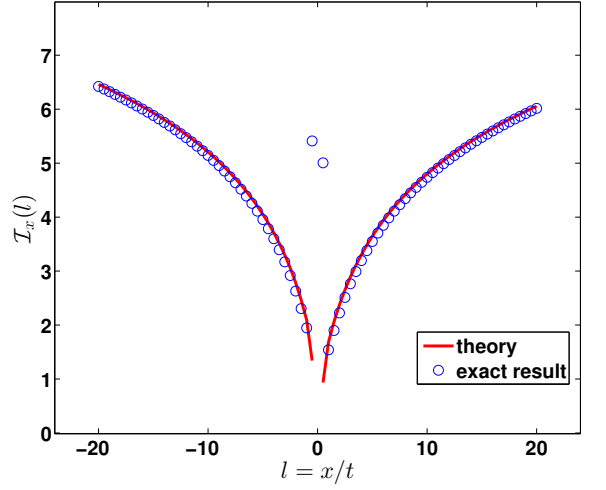


FIG. 8: Rate function $\mathcal{I}_x(l)$, where the waiting time follows Erlang distribution $\phi(\tau) = \tau^{m-1} \exp(-\tau)/(m-1)!$ with $m = 2$. Here the solid line shows theoretical prediction Eq. (62) and the related exact results is obtained from Eqs. (1) and (34) with $Q_t(N) = (\Gamma(2N+2, t)/\Gamma(2N+2) - \Gamma(2N, t)/\Gamma(2N)$ [33], where $\Gamma(x, y)$ is the complete gamma function. The parameters are $t = 2$, $p = 0.6$ and $q = 0.4$.

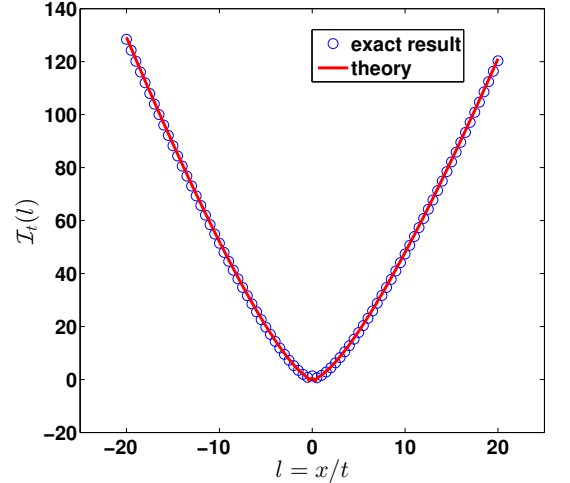


FIG. 9: Time Rate function $\mathcal{I}_t(l)$. The solid line shows the plot of Eq. (65), and the symbols illustrate the exact results. The parameters are the same as in Fig. 8.

statistics of the waiting-time distribution near the origin rather than by its tail. This behavior is markedly different from that of typical fluctuations, which govern the central part of the position distribution and are, for example, described by Lévy stable laws originating from the tail of the waiting-time PDF. Based on Figs. 2 and 5, the far tails are sensitive to the disturbance of the system even when the observation time is short.

In [37], the detailed balance assumption was discussed.

Clearly, Gaussian distribution satisfies this assumption, i.e., $f(x)/f(-x) = \exp(2xa/\sigma^2)$. Based on Eq. (16), there exists

$$\ln \left(\frac{P(x, t)}{P(-x, t)} \right) \sim 2 \frac{a}{\sigma^2} x, \quad (66)$$

showing the linear relationship with the position x . Note that Eq. (66) is the exact result using the method given in [37]. Similarly, utilizing Eq. (56), for the discrete case the ratio between two tails yields $P(|x|, t)/P(-|x|, t) \sim (p/q)^{|x|}$. Recalled that these relations are independent of the statistics of waiting times, indicating that Eq. (66) may have potential applications in experiments.

Throughout the manuscript, we restrict ourselves to waiting-time distributions that are analytic at small τ , as given by Eq. (3). A natural question is what changes when the waiting times are instead drawn from the one-sided Lévy distribution. At least according to numer-

ical simulations, the far tails of the positional distribution decay faster than an exponential function. For the non-analytic case, the rate-function approach developed by Sokolov and Pacheco [34] may offer advantages over saddle-point methods. Besides, it also interesting to discuss the convergence problem for the mentioned two methods when the bias is added.

Acknowledgments

W.W. thanks Eli Barkai and Stanislav Burov for their insightful discussions and for motivating this work. W.W. was supported by the National Natural Science Foundation of China under Grant No. 12105243 and the Zhejiang Province Natural Science Foundation LQ22A050002.

[1] S. N. Majumdar and M. Vergassola, Large deviations of the maximum eigenvalue for wishart and Gaussian random matrices, *Phys. Rev. Lett.* **102**, 060601 (2009).

[2] R. Lefevere, M. Mariani, and L. Zambotti, Large deviations for renewal processes, *Stoch. Process. Their Appl.* **121**, 2243 (2011).

[3] H. Touchette, Introduction to dynamical large deviations of markov processes, *Physica A* **504**, 5 (2018), lecture Notes of the 14th International Summer School on Fundamental Problems in Statistical Physics.

[4] A. G. Cherstvy, S. Thapa, C. E. Wagner, and R. Metzler, Non-gaussian, non-ergodic, and non-Fickian diffusion of tracers in mucin hydrogels, *Soft Matter* **15**, 2526 (2019).

[5] W. Wang, M. Höll, and E. Barkai, Large deviations of the ballistic lévy walk model, *Phys. Rev. E* **102**, 052115 (2020).

[6] L. Defaveri, E. Barkai, and D. A. Kessler, Stretched-exponential relaxation in weakly-confined Brownian systems through large deviation theory (2023).

[7] P. Chaudhuri, L. Berthier, and W. Kob, Universal nature of particle displacements close to glass and jamming transitions, *Phys. Rev. Lett.* **99**, 060604 (2007).

[8] R. Hou, A. G. Cherstvy, R. Metzler, and T. Akimoto, Biased continuous-time random walks for ordinary and equilibrium cases: facilitation of diffusion, ergodicity breaking and ageing, *Phys. Chem. Chem. Phys.* **20**, 20827 (2018).

[9] R. Metzler and J. Klafter, The random walk's guide to anomalous diffusion: a fractional dynamics approach, *Phys. Rep.* **339**, 1 (2000).

[10] W. Deng, R. Hou, W. Wang, and P. Xu, *Modeling Anomalous Diffusion: From Statistics to Mathematics* (World Scientific, Singapore, 2020).

[11] W. Wang and E. Barkai, Fractional advection-diffusion-asymmetry equation, *Phys. Rev. Lett.* **125**, 240606 (2020).

[12] G. Afek, N. Davidson, D. A. Kessler, and E. Barkai, Colloquium: Anomalous statistics of laser-cooled atoms in dissipative optical lattices, *Rev. Mod. Phys.* **95**, 031003 (2023).

[13] T. J. Lampo, S. Stylianidou, M. P. Backlund, P. A. Wiggins, and A. J. Spakowitz, Cytoplasmic rna-protein particles exhibit non-Gaussian subdiffusive behavior, *Biophys. J.* **112**, 532 (2017).

[14] C. Xue, X. Zheng, K. Chen, Y. Tian, and G. Hu, Probing non-gaussianity in confined diffusion of nanoparticles, *J. Phys. Chem.* **7**, 514 (2016).

[15] K. He, F. Babaye Khorasani, S. T. Rettner, D. K. Thomas, J. C. Conrad, and R. Krishnamoorti, Diffusive dynamics of nanoparticles in arrays of nanoposts, *ACS Nano* **7**, 5122 (2013), pMID: 23672180.

[16] S. K. Ghosh, A. G. Cherstvy, and R. Metzler, Non-universal tracer diffusion in crowded media of non-inert obstacles, *Phys. Chem. Chem. Phys.* **17**, 1847 (2015).

[17] B. Wang, S. M. Anthony, S. C. Bae, and S. Granick, Anomalous yet Brownian, *Proc. Natl. Acad. Sci. U.S.A.* **106**, 15160 (2009).

[18] J. Masoliver, M. Montero, and J. M. Porrà, A dynamical model describing stock market price distributions, *Physica A* **283**, 559 (2000).

[19] S. Hapca, J. W. Crawford, and I. M. Young, Anomalous diffusion of heterogeneous populations characterized by normal diffusion at the individual level, *J. R. Soc. Interface* **6**, 111 (2009).

[20] N. Schramma, C. Perugachi Israëls, and M. Jalaal, Chloroplasts in plant cells show active glassy behavior under low-light conditions, *Proceedings of the National Academy of Sciences* **120**, e2216497120 (2023).

[21] L. Luo and M. Yi, Quenched trap model on the extreme landscape: The rise of subdiffusion and non-gaussian diffusion, *Phys. Rev. E* **100**, 042136 (2019).

[22] W. K. Kegel and A. van Blaaderen, Direct observation of dynamical heterogeneities in colloidal hard-sphere suspensions, *Science* **287**, 290 (2000).

[23] E. R. Weeks, J. C. Crocker, A. C. Levitt, A. Schofield, and D. A. Weitz, Three-dimensional direct imaging of structural relaxation near the colloidal glass transition, *Science* **287**, 627 (2000).

[24] K. C. Leptos, J. S. Guasto, J. P. Gollub, A. I. Pesci, and R. E. Goldstein, Dynamics of enhanced tracer diffusion in suspensions of swimming eukaryotic microorganisms, *Phys. Rev. Lett.* **103**, 198103 (2009).

[25] C. Eisenmann, C. Kim, J. Mattsson, and D. A. Weitz, Shear melting of a colloidal glass, *Phys. Rev. Lett.* **104**, 035502 (2010).

[26] T. Toyota, D. A. Head, C. F. Schmidt, and D. Mizuno, Non-gaussian athermal fluctuations in active gels, *Soft Matter* **7**, 3234 (2011).

[27] M. J. Skaug, J. Mabry, and D. K. Schwartz, Intermittent molecular hopping at the solid-liquid interface, *Phys. Rev. Lett.* **110**, 256101 (2013).

[28] D. Wang, H. Wu, and D. K. Schwartz, Three-dimensional tracking of interfacial hopping diffusion, *Phys. Rev. Lett.* **119**, 268001 (2017).

[29] R. Jeanneret, D. O. Pushkin, V. Kantsler, and M. Polin, Entrainment dominates the interaction of microalgae with micron-sized objects, *Nat. Commun.* **7**, 12518 (2016).

[30] A. V. Chechkin, F. Seno, R. Metzler, and I. M. Sokolov, Brownian yet non-gaussian diffusion: From superstatistics to subordination of diffusing diffusivities, *Phys. Rev. X* **7**, 021002 (2017).

[31] M. Hu, H. Chen, H. Wang, S. Burov, E. Barkai, and D. Wang, Triggering gaussian-to-exponential transition of displacement distribution in polymer nanocomposites via adsorption-induced trapping, *ACS Nano* **17**, 21708 (2023).

[32] E. Barkai and S. Burov, Packets of diffusing particles exhibit universal exponential tails, *Phys. Rev. Lett.* **124**, 060603 (2020).

[33] W. Wang, E. Barkai, and S. Burov, Large deviations for continuous time random walks, *Entropy* **22**, 697 (2020).

[34] A. Pacheco-Pozo and I. M. Sokolov, Large deviations in continuous-time random walks, *Phys. Rev. E* **103**, 042116 (2021).

[35] O. Hamdi, S. Burov, and E. Barkai, Laplace's first law of errors applied to diffusive motion, *The European Physical Journal B* **97**, 1 (2024).

[36] J. M. Miotto, S. Pigolotti, A. V. Chechkin, and S. Roldán-Vargas, Length scales in brownian yet non-gaussian dynamics, *Phys. Rev. X* **11**, 031002 (2021).

[37] S. Burov, W. Wang, and E. Barkai, Exponential tails and asymmetry relations for the spread of biased random walks, *arXiv:2209.03410*.

[38] H. Touchette, The large deviation approach to statistical mechanics, *Phys. Rep.* **478**, 1 (2009).

[39] S. Whitelam, Large deviations in the presence of cooperativity and slow dynamics, *Phys. Rev. E* **97**, 062109 (2018).

[40] A. Vezzani, E. Barkai, and R. Burioni, Single-big-jump principle in physical modeling, *Phys. Rev. E* **100**, 012108 (2019).

[41] W. Wang, A. Vezzani, R. Burioni, and E. Barkai, Transport in disordered systems: The single big jump approach, *Phys. Rev. Res.* **1**, 033172 (2019).

[42] A. Vezzani, E. Barkai, and R. Burioni, Rare events in generalized lévy walks and the big jump principle, *Sci. Rep.* **10**, 2732 (2020).

[43] A. Vezzani and R. Burioni, Fast rare events in exit times distributions of jump processes, *Phys. Rev. Lett.* **132**, 187101 (2024).

[44] C. Godrèche and J. M. Luck, Statistics of the occupation time of renewal processes, *J. Stat. Phys.* **104**, 489 (2001).

[45] W. Wang, J. H. P. Schulz, W. H. Deng, and E. Barkai, Renewal theory with fat-tailed distributed sojourn times: Typical versus rare, *Phys. Rev. E* **98**, 042139 (2018).

[46] W. Wang and S. Burov, Statistics of a large number of renewals in equilibrium and non-equilibrium renewal processes (2024).

[47] H. E. Daniels, Saddlepoint approximations in statistics, *Ann. Math. Statist.* **25**, 631 (1954).

[48] R. M. Corless, G. H. Gonnet, D. E. G. Hare, D. J. Jeffrey, and D. E. Knuth, On the Lambert *W* function, *Adv. Comput. Math.* **5**, 329 (1996).

[49] L. Zarfaty and B. Meerson, Statistics of large currents in the kipnis–marchioro–presutti model in a ring geometry, *J. Stat. Mech: Theory Exp.* **2016**, 033304 (2016).

[50] L. Zarfaty, A. Peletskyi, I. Fouxon, S. Denisov, and E. Barkai, Dispersion of particles in an infinite-horizon lorentz gas, *Phys. Rev. E* **98**, 010101 (2018).

[51] E. Barkai and Y. C. Cheng, Aging continuous time random walks, *J. Chem. Phys.* **118**, 6167 (2003).

[52] J. Klafter and I. M. Sokolov, *First Steps in Random Walks: From Tools to Applications* (Oxford University Press, Oxford, 2011).

[53] W. L. Wang and W. H. Deng, Aging Feynman-Kac equation, *J. Phys. A* **51**, 015001 (2018).

[54] G. Gradenigo, A. Sarracino, D. Villamaina, and A. Vulpiani, Einstein relation in superdiffusive systems, *J Stat Mech: Theory Exp* **2012**, L06001 (2012).

[55] D. Nickelsen and H. Touchette, Anomalous scaling of dynamical large deviations, *Phys. Rev. Lett.* **121**, 090602 (2018).

[56] K. Pearson, The problem of the random walk, *Nature* **72**, 342 (1905).